

VALIDATION OF THE PYROLYSIS MODEL OF FDS 6 FOR A LARGE-SCALE ETHANOL POOL FIRE

S. Ebrahim Zadeh, T. Beji and B. Merci

Setareh.Ebrahimzadeh@UGent.be

Ghent University-UGent, Department of Flow, Heat and Combustion Mechanics,
Sint-Pietersnieuwstraat 41, Ghent, Belgium

Abstract

A numerical study has been performed on the prediction of the burning rate (and thus the Heat Release Rate, HRR) of a large-scale Ethanol pool fire ($0.81m \times 0.70m$) using the Fire Dynamics Simulator (FDS 6). The study has shown that the steady-state burning rate is reasonably well predicted and the results are relatively insensitive to the mesh resolution when cells of 5 cm and 2.5 cm are employed. Furthermore, it has been shown numerically that the lip height could increase up to 50 % the burning rate in comparison to the *flush* configuration (i.e. no lip) as found in a previous experimental study. Finally, a simple 1-D calculation using FDS 6 has confirmed that the incident radiative flux on the fuel surface is the dominant heat transfer mode and contributes by approximately 70% in the fuel burning rate.

Introduction

Despite the continuing advances in turbulence and combustion modelling and the increasing computational resources, liquid-pool fire in well-ventilated open atmosphere conditions remain a challenging scenario to be modelled. The complexity of such scenario stems from the strong coupling and interaction between several aspects of the problem such as combustion, turbulence, radiation and pyrolysis. A large body of the literature devoted to such configuration has focused on the combustion (near-field) and plume (far-field) regions by (1) giving insight into the development of the flow field via experimental testing (e.g. [1]), and (2) exploring the numerical modelling capabilities by prescribing the fuel Mass Loss Rate (MLR) or evaporation rate (e.g.[2]). Fewer studies (e.g. [3]) have addressed the predictive capabilities of the MLR by performing fully coupled mass and heat transfer calculations at the liquid pool surface. More specifically, in [3] the authors have used Large Eddy Simulation (LES) for the turbulent flow field and a Finite Volume Method (FVM) to solve the Radiative Transfer Equation (RTE) in order to simulate Methanol pool fires with diameters between 0.01 and 1 m. The simulations provided well the qualitative dependence between the pool size and the burning rate. However, the deviations between measured and predicted data for the burning rate ranged between 37 and 120 %. Therefore, the authors recommended that further validation studies should be carried out, which is the main objective of the present work.

The paper presents a validation study of the pyrolysis model implemented in the Fire Dynamics Simulator (FDS 6), a Computational Fluid Dynamics (CFD) code developed by the National Institute of Standards and Technology (NIST) for low Mach number flows driven by combustion heat release and buoyancy ([4] and [5]). It is hence widely used in the fire safety community. The test case considered hereafter consists of a large-scale ($0.81m \times 0.70m$) Ethanol pool fire experiment performed by Thomas et al.[6].

Numerical modelling

In FDS 6, the Navier-Stokes equations are solved using a second-order finite differences numerical scheme with a low Mach number formulation. The main combustion model

is based on the mixture fraction concept with infinitely fast chemistry. The turbulence model is based on LES with four available models for the turbulent viscosity: Deardorff, Vreman, constant Smagorinsky and dynamic Smagorinsky. The former is the default model. The RTE is solved using FVM. A radiative fraction, χ_R , is prescribed (by default) as an upper bound in order to limit the uncertainties in the radiation calculation induced by uncertainties in the temperature field. In the current work the radiative fraction for Ethanol is taken as $\chi_R = 0.18$ (an average of the values suggested in [7] and [8]). Heat losses to the walls are computed by solving the 1-D Fourier's equation for conduction. Except where mentioned, all the default constants in FDS have been used. More modelling details are provided hereafter regarding liquid pyrolysis.

Although the necessary details regarding the pyrolysis model are provided in [5], they are repeated here for the sake of completeness. The 1-D heat conduction equation for the temperature T_ℓ of the liquid layer is expressed as:

$$\rho_\ell c_\ell \frac{\partial T_\ell}{\partial t} = \frac{\partial}{\partial x} \left(k_\ell \frac{\partial T_\ell}{\partial x} \right) + \dot{q}_\ell''' \quad (1)$$

where ρ_ℓ , c_ℓ and k_ℓ are respectively the density, specific heat and conductivity of the liquid. All three parameters are taken here as constants. The source term \dot{q}_ℓ''' consists of the sum of chemical reactions and radiative absorption:

$$\dot{q}_\ell''' = \dot{q}_{\ell,c}''' + \dot{q}_{\ell,r}''' \quad (2)$$

The surface temperature of the liquid, $T_{\ell,x=0}$, by solving the following boundary condition:

$$-k_\ell \left(\frac{\partial T_\ell}{\partial x} \right)_{x=0} = \dot{q}_c'' + \dot{q}_r'' \quad (3)$$

where \dot{q}_c'' and \dot{q}_r'' are respectively the convective and radiative fluxes at the surface.

A two flux model is used to compute the radiative intensity based on the assumption that the latter is constant inside the forward and the backward hemispheres.

The radiative source term, $\dot{q}_{\ell,r}'''$, in the heat conduction equation, is the sum of the forward and backward flux gradients:

$$\dot{q}_{\ell,r}'''(x) = \frac{d\dot{q}_r^+(x)}{dx} + \frac{d\dot{q}_r^-(x)}{dx} \quad (4)$$

The forward radiative heat flux into the liquid is computed according to:

$$\frac{1}{2} \frac{d\dot{q}_r^+(x)}{dx} = \kappa_\ell (\sigma T_\ell^4 - \dot{q}_r^+(x)) \quad (5)$$

where κ_ℓ is the absorption coefficient of the liquid taken as constant.

A similar equation is computed for the backward radiative heat flux.

The boundary condition for the previous equation at the liquid surface, i.e. $x = 0$, reads:

$$\dot{q}_{r,x=0}''+ = \dot{q}_{r,in}'' + (1 - \varepsilon) \dot{q}_{r,x=0}''- \quad (6)$$

where ε is the emissivity at the liquid surface (taken as constant) and $\dot{q}_{r,in}''$ is the incoming radiative flux, which is directly proportional to the emissivity.

The convective heat flux, \dot{q}_c'' , is calculated according to the following expression:

$$\dot{q}_c'' = h (T_g - T_{\ell,x=0}) \quad (7)$$

where h is the convection coefficient and T_g is the gas temperature near the surface. The

convective heat transfer coefficient is calculated based on a combination of natural and forced convection correlations [5].

The volume fraction of the fuel vapor above the surface is expressed using the Clausius-Clapeyron relation:

$$X_{F,\ell} = \exp \left[-\frac{h_v W_F}{R} \left(\frac{1}{T_{\ell,x=0}} - \frac{1}{T_b} \right) \right] \quad (8)$$

where h_v is the heat of vaporization of the liquid (i.e. the fuel), W_F its molecular weight and T_b its boiling temperature. The parameter R denotes the universal gas constant.

The evaporation rate of the fuel is expressed as:

$$\dot{m}_{vapor}'' = h_m \frac{\bar{p}_m W_F}{R T_g} \ln \left(\frac{X_{F,g} - 1}{X_{F,\ell} - 1} \right) \quad (9)$$

where h_m is the mass transfer coefficient, \bar{p}_m is the pressure, and $X_{F,g}$ is the volume fraction of fuel vapor in the grid cell adjacent to the pool surface. The mass transfer number is a function of the Sherwood number, a specified length scale and a liquid-gas diffusion coefficient (see [5] for more details).

All the required thermochemical properties of Ethanol for the simulation presented here are listed in Table 1.

Table 1: Thermochemical properties of Ethanol used in the numerical simulation

Property	Symbol	Value	Reference
Heat of combustion (kJ/kg)	ΔH_c	26780	[9]
Combustion efficiency (-)	χ	0.97	[6]
Heat of vaporization(kJ/kg)	h_v	838	[9]
Boiling point ($^{\circ}C$)	T_b	78.5	[9]
Absorption coefficient (m^{-1})	κ_{ℓ}	1534.3	[10]
Emissivity (-)	ε_{ℓ}	1	Assumption
Density (kg/m^3)	ρ_{ℓ}	789	[9]
Specific heat (kJ/kg.K)	c_{ℓ}	2.44	[11]
Conductivity (W/m.K)	k_{ℓ}	0.17	[11]

Case description and computational set-up

The large-scale Ethanol pool fire considered in this study has been experimentally studied by Thomas et al [6]. The fuel tray was of $0.81m \times 0.70m \times 0.05m$ size constructed from steel with thickness of 3 mm. A volume of 5 liter standard commercial grade methylated spirit consisting of 97 % ethanol and 3 % water was used as fuel. This volume corresponds

to an initial fuel depth of 8.82 mm . It is important to note that the initial fuel surface is not *flush* to the height of the tray, there is indeed a lip (also referred to in the literature as freeboard or bounding rim above fuel level) with a height of approximately 4 cm . The tray was placed directly under the hood of a calorimeter and the temporal HRR profile was measured. The computational domain is set with the following dimensions: $3\text{ m} \times 3\text{ m} \times 4\text{ m}$ (see Fig. 1). The width of the domain ensures minimal influence of the *open* boundary conditions (at the sides) on the air entrainment near the fire. The height of the domain is set to be almost three times the expected flame height to allow a fully developed fire plume by defining an *open* boundary condition. All the simulations in this study were performed with a uniform structured mesh. In the grid sensitivity study three cells sizes were considered: 10 cm , 5 cm and 2.5 cm .

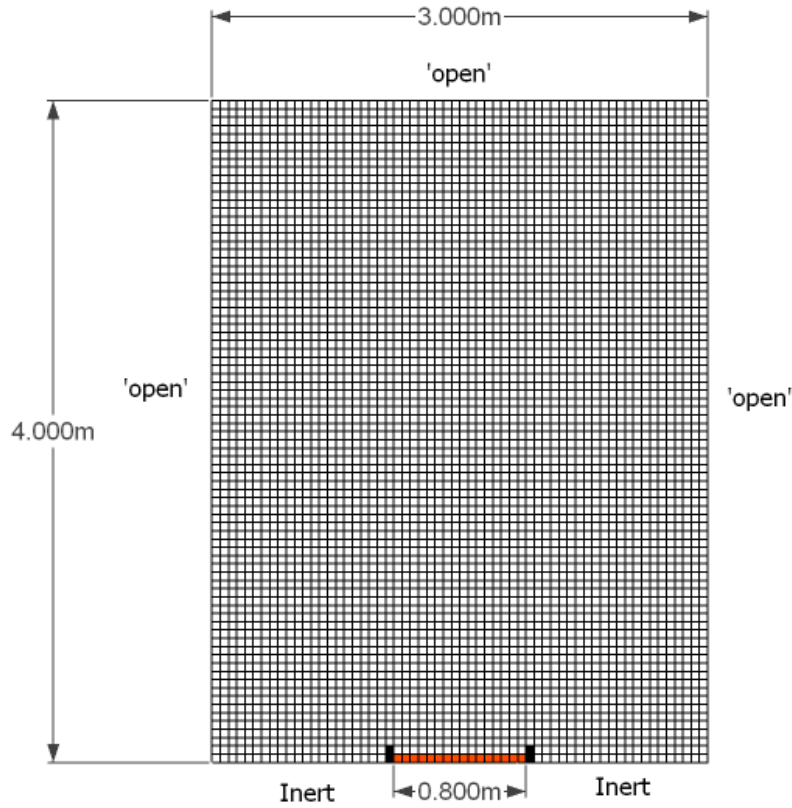


Figure 1: Computational domain, mesh (cell size of 5 cm) and boundary conditions for the studied case.

Results

The results are examined in terms of:

1. grid sensitivity,
2. comparison to the experimental results and rim effect, and
3. analysis of the radiative feedback to the fuel surface.

and verification for the liquid phase only.

Grid sensitivity: The results for the grid sensitivity study displayed in Fig. 2 show that the steady-state HRR for the 10 cm grid is approximately 36% lower than for the 5 cm grid. When refining the cell size to 2.5 cm , no significant difference is found with the 5

cm grid. Therefore, 5 cm was considered as an appropriate cell size and the corresponding mesh was selected for a complementary simulation on the rim effect as explained hereafter.

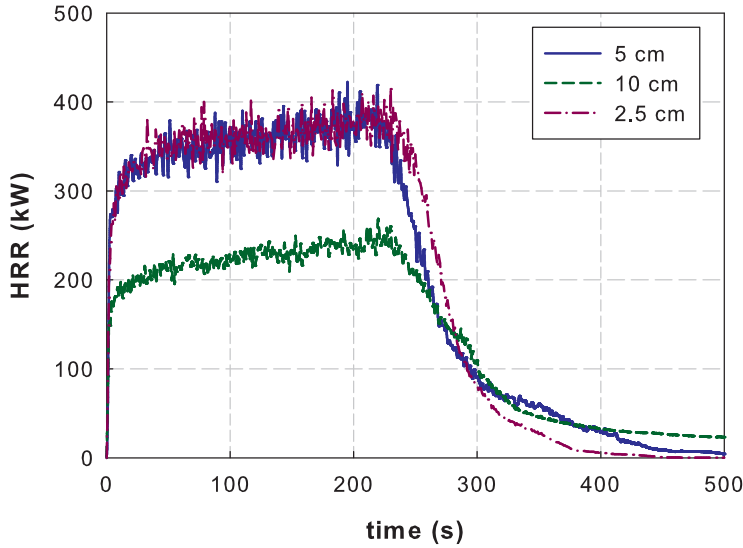


Figure 2: Results of the grid sensitivity study.

Comparison to the experimental data and rim effect: Figure 3 shows that the initial transient stage and decay stages in the HRR profile are not well reproduced by the simulation. A steady-stage is reached faster and over a longer period in the simulation (i.e. [20 s - 200 s]) in comparison to the experimental profile (i.e. [150 s - 300 s]). This discrepancy could be partly described by the fact that the ignition process has not been modeled in the current simulation, meaning that the whole fuel bed area is ignited from the start. In the experiment, it is possible that some time might have been required before the flame area at its base spans fully over the liquid surface. However, the steady-state HRR values compare well: 350 kW for the simulation and 375 kW for the experiment.

Comparison to an empirically-derived correlation and rim effect: The predicted and measured steady-state HRR are also compared to the value obtained from the empirically-derived correlation [12] where the burning rate per unit area is expressed as:

$$\dot{m}'' = \dot{m}''_{\infty} (1 - e^{-KD}) \quad (10)$$

where \dot{m}''_{∞} is the limiting burning rate, K the extinction coefficient and D the pool diameter. The reported burning rate for Ethanol is $\dot{m}'' = \dot{m}''_{\infty} = 0.015 \text{ kg/m}^2.\text{s}$ and is independent of the diameter due to the low amounts of soot produced and the absence of a measured extinction coefficient K . The burning rate corresponds for the studied pool diameter to a steady-state Heat Release Rate of

$$\dot{Q} = \chi A_F \dot{m}'' \Delta H_c = 221 \text{ kW}$$

where A_F is the pool area.

This relatively low value in comparison to the other two values can be explained by the fact that for the case at hand there is a bounding rim above fuel level. In [13], it has been found that the burning rate increases as the bounding rim increases (i.e. increased lip height) above fuel level. Figure 3 shows that this effect is captured numerically by the FDS simulation.

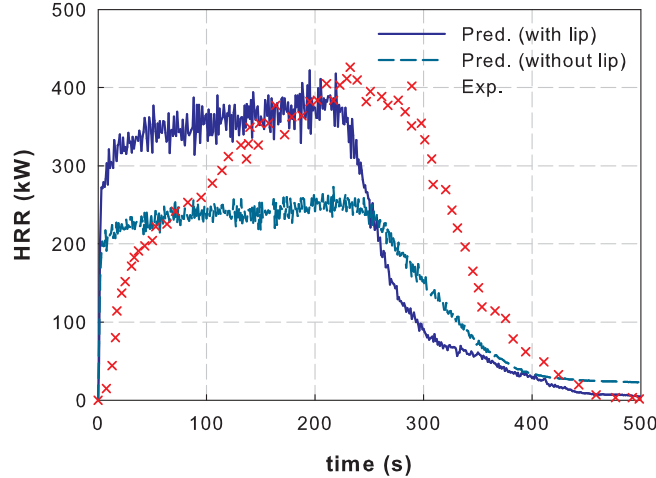


Figure 3: Comparison of the predicted HRR profile (with and without lip) against the experimental data.

Radiative feedback to the fuel surface: The radiative heat feedback to the fuel surface in liquid pool fires is a mechanism which plays a dominant role in the determination of burning rates. Klassen and Gore [14] performed a series of experimental measurements and calculations of the flame radiative heat flux to the pool surface for several liquid-fuelled flames. For example, the radiative heat flux incident the surface of a 30 cm Toluene pool fire was around 36 kW/m^2 . It did not vary significantly from the centreline up to radial position of $r = 0.2D$. Calculations for the same flame based on energy balance at the liquid surface have shown that a radiative flux of approximately 30 to 32 kW/m^2 is sufficient to maintain the observed burning rate of $\dot{m}'' = 0.0431 \text{ kg/m}^2 \cdot \text{s}$. More generally, it has been reported in [15] that for pool diameters higher than 0.25 m, the contribution of radiative heat transfer increases substantially with pool diameter. For example, the convective component of the flame flux to the pool surface decreases from about 54 to 5% as pool diameter increases from 0.15 to 0.50 m. Convective heat transfer is the main mode of heat transfer for pool fires with diameters less than 0.2 m.

For the case at hand in this study (where the hydraulic diameter is 0.75 m) we clearly expect, according to the findings stated earlier, the incident radiative heat flux on the pool surface to be the dominant heat transfer and the main contributor to the burning rate. Unfortunately, experimental measurements of the incident radiative heat flux to the pool surface for the case of interest are not available. However, numerically predicted values have been recorded. Figure 4 shows that the peak radiative heat flux of around 20 kW/m^2 occurs at the centreline and decreases slightly towards the edge of the fuel tray to a value of 8 kW/m^2 . The average incident radiative heat flux over the whole liquid surface is 14.31 kW/m^2 . In order to estimate the contribution of the latter in the observed burning rate corresponding to a HRR of 375 kW (as done in [14]), a simple 1-D calculation has been performed in FDS 6. In such calculation, the following steps are considered:

1. The gas phase (and more specifically combustion) is turned off by setting and ambient oxygen concentration to a value which is too low to support any burning (e.g. $Y_{O_2, \infty} = 0.01 \text{ g/g}$),
2. Convective heat transfer between the liquid surface and the gas is turned off by setting the convective coefficient to $h = 0 \text{ kW/m}^2 \cdot \text{K}$, and,

3. An external heat flux at the surface of the liquid is applied with a value of 14.31 kW/m^2 equal to the predicted radiative heat flux in the main simulation.

Such approach is used experimentally to derive for example the heat of gasification of fluids by applying heat fluxes in the range of 10 to 60 kW/m^2 in air with less than 10 % of oxygen concentration [7]. The calculation procedure is also recommended in the Users' Guide of FDS in order to eliminate uncertainties related to convection, combustion and apparatus specific phenomena [4]. It has been found that the radiative heat flux of 14.31 kW/m^2 on the liquid surface leads to a burning rate of $\dot{m}'' = 0.016 \text{ kg/m}^2 \cdot \text{s}$ (equivalent to a HRR of 240 kW) that represents 70 % of the experimental value. This finding confirms that the dominance and contribution of the radiative heat transfer mode in the burning rate is well predicted by FDS 6.

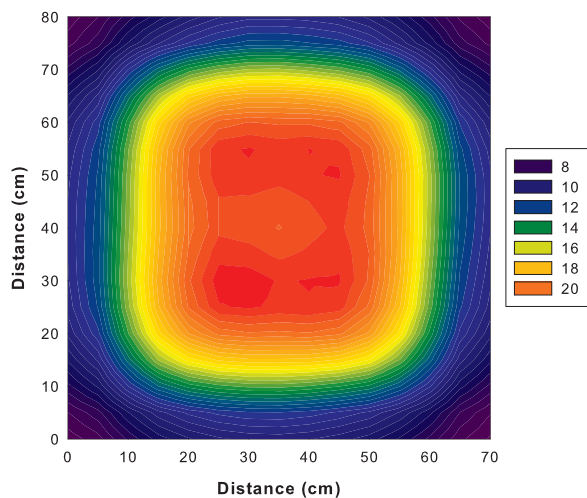


Figure 4: Contour plot of the predicted incident radiative heat flux (in kW/m^2) on the pool surface.

Conclusions

The liquid pyrolysis model in FDS 6 has provided a good prediction of the burning rate of a $0.81\text{m} \times 0.7\text{m}$ Ethanol pool fire. A grid sensitivity analysis has shown that the results are relatively grid insensitive when a cell size of 5 or 2.5 cm is used. The lip height has proven to be an important element in the burning rate prediction. In a complementary simulation with a *flush* configuration, the predicted burning rate was 50 % lower than the actual experimental rate. This is in accordance with experimental findings in [13]. A simple 1-D calculation using FDS has confirmed that FDS 6 predicts well that the dominance and contribution of the radiative heat transfer mode in the burning rate.

The results obtained during this study constitute an encouraging step towards fully predictive capabilities of pool fires. The choice of an Ethanol fire was mainly motivated by the relatively low soot concentrations. In future studies sootier fuels such as Heptane and Toluene must be addressed. This task remains however very challenging due to the numerous complexities inherent to soot modelling such as for instance the presence of cool unburned sooty pyrolysis gases near the surface, which hinders part of the flame radiation to the fuel surface and thus affects directly the burning rate.

Acknowledgment

This research was funded by the Scientific Fund for Research Flanders (Belgium) (FWO-Vlaanderen) through project 3G004912.

Nomenclature

A_F	fuel area
c	specific heat
D	diameter
h	convective coefficient
h_m	mass transfer coefficient
h_v	heat of vaporization
K	extinction coefficient
k	conductivity
\dot{m}''	mass loss rate per unit area
\bar{p}_m	pressure
\dot{Q}	fire Heat Release Rate (HRR)
\dot{q}''	heat flux
\dot{q}'''	heat source term
R	universal gas constant
T	temperature
t	time
W_F	fuel molecular weight
X_F	volume fraction of fuel
x	vertical distance from liquid surface
$Y_{O_2,\infty}$	ambient oxygen mass concentration
ΔH_c	heat of combustion
ϵ	emissivity
κ	absorption coefficient
ρ	density
χ	combustion efficiency

Subscripts

b	boiling
c	convective
g	gas
in	incoming
l	liquid
r	radiative
$vapor$	vapor
∞	limiting burning rate

Superscripts

$+$	forward direction
$-$	backward direction

References

- [1] Weckman, E., Strong, A., “Experimental investigation of the turbulence structure interaction of medium-scale methanol pool fire”, *Proc. Comb. Inst.* 105:245–266 (1996).
- [2] Wen, J., Kang, K., Donchev, T., Karwatzki, J., “Validation of fds for the prediction of medium-scale pool fires”, *Fire Safety and J.* 42:127–138 (2007).
- [3] Hostikka, S., McGrattan, K., Hamins, A., “Numerical modeling of pool fires using les and finite volume method for radiation”, *Proc 7th International Symposium on Fire Safety Science*, Worcester, MA, USA, pp. 383–394.

- [4] McGrattan, K., Hostikka, S., McDermott, R., Floyd, J., Weinschenk, C., Overholt, K., “Fire dynamics simulator (version6), users’ guide”, *NIST special publication* (2013).
- [5] McGrattan, K., Hostikka, S., McDermott, R., Floyd, J., Weinschenk, C., Overholt, K., “Fire dynamics simulator (version6), technical guide”, *NIST special publication* (2013).
- [6] Thomas, I., Khalid, A., Moinuddin, K., Bennetts, I., “The effect of fuel quantity and location on small enclosure fires”, *J. Fire. Prot. Eng.* 17:85–102 (2007).
- [7] Tewarson, A., *The SFPE handbook of Fire Protection Engineering*, National Fire Protection Association, 2002, chapter 3-4, Generation of Heat and Chemical Compounds in Fires, p. 3-111.
- [8] Gore, J., Klassen, M., Hamins, A., Kashiwagi, T., “Fuel property effects on burning rate and radiative transfer from liquid pool flames”, *Proc 3rd International Symposium on Fire Safety Science*, Borehamwood, UK, pp. 395–404.
- [9] Drysdale, D., *An Introduction to Fire Dynamics*, Wiley, 2001.
- [10] Suo-Anttila, J., Blanchat, T., Ricks, A., Brown, A., “Characterization of thermal radiation spectra in 2 m pool fires”, *Proc. Comb. Inst.* 32:2567–2574 (2009).
- [11] www.engineeringtoolbox.com .
- [12] Babrauskas, V., *The SFPE handbook of Fire Protection Engineering*, National Fire Protection Association, 2002, chapter 3-1, Heat Release Rates.
- [13] Bouhafid, A., Vantelon, J., Joulain, P., Fernandez-Pello, A., “On the flame structure at the base of a pool fire”, *Proc. Comb. Inst.* 22:1291–1298 (1988).
- [14] Gore, J., Klassen, M., “Structure and radiation properties of pool fires”, *NIST Report, NIST-GCR-94-651* (1994).
- [15] Joulain, P., “The behaviour of pool fires: State of the art and new insights”, *Proc. Comb. Inst.* 27:2691–2706 (1998).